ChemComm

Accepted Manuscript

This article can be cited before page numbers have been issued, to do this please use: X. Zhang, X. Tan, D. Zhang, N. Liao, Y. Zheng, A. Zheng, Y. Zeng, X. Liu and J. Liu, *Chem. Commun.*, 2017, DOI: 10.1039/C7CC05295B.

ROYAL SOCIETY OF CHEMISTRY

rsc.li/chemcomm

ROYAL SOCIETY OF CHEMISTRY View Article Online
DOI: 10.1039/C7CC05295B

Journal Name

COMMUNICATION

A cancer cell specific targeting nanocomplex for combination of mRNA-responsive photodynamic and chemo-therapy

Received 00th January 20xx,
Accepted 00th January 20xx

DOI: 10.1039/x0xx00000x

www.rsc.org/

Xiaolong Zhang[a,b], Xionghong Tan[c], Da Zhang[a,b], Naishun Liao[a,b], Youshi Zheng[a,b], Aixian Zheng[a,b], Yongyi Zeng[a,b,d], Xiaolong Liu[a,b,*] and Jingfeng Liu[a,b,d*]

We have developed a cancer cell specific targeting nanocomplex which combines the photodynamic therapy with chemotherapy through precisely responding to the intracellular tumor-related mRNA. The combined treatment of these two modalities showed a significantly enhanced therapeutic effects on cancer cells.

Photodynamic therapy (PDT), one of promising treatment modality, combines photosensitizers (PS) and light irradiation to generate reactive oxygen species (ROS) for treating various diseases including cancer.[1,2] PDT shows excellent selectivity to local tissues by controlling the light illumination, and avoids severe side effects comparing with conventional chemotherapy.[3] However, the limited tumor selectivity of PSs leads to nonspecific activation of ROS in normal tissues upon light excitation.[4] Additionally, the PDT always accompanies with tissue oxygen consuming and resulting in severe hypoxia, leading to lower treatment efficacy.[2] The integrating of chemotherapy and PDT may be a promising strategy to overcome the drawbacks of PDT. Multifunctional nanoparticle based drug delivery systems (DDS) have shown bright prospect in cancer therapy owing to the improved drug bioactivity and bioavailability.[5,6] Currently, various stimuli have been developed to design smart DDS, such as, temperature,[7] light[8], pH,[9] enzyme,[10] redox[11] and biomolecules.[12] Notably, integration of active targeting and stimuli-responsive ability to DDS can enhance the tumor specific accumulation and therapeutic efficacy of drugs. Such type of nanocarriers can specifically accumulate at the tumor sites and be controlled to precisely release drugs in target tumor cells. Therefore, the design of tumor specific targeting nanocarriers, that combine the PDT and chemotherapy with stimuli-responsive ability, might be a helpful strategy for increase the therapeutic efficiency.[13]

Tumor related mRNA as a specific biomarker is closely associated with the development of tumor, and can be used to monitor tumor progression and assess treatment outcome.[14] Meanwhile, the tumor related mRNA also can be used as a promising endogenous specific stimulus for designing of DNA rehybridization-related imaging probes and smart drugs.[15,16] Nowadays, a number of nanoparticles have been development as theranostic nanoagents based on mRNA as trigger or stimulus, such as gold nanoparticles,[17] quantum dots[18] and graphene oxide,[19] etc.[20,21] Although these nanoagents have shown excellent beneficial outcomes, most of these agents contain nonbiodegradable components and need complicated chemical synthesis and conjugation procedures, as well as sophisticated design. Hence, there is still an urgent need for developing novel completely biodegradable nanocarriers with simple fabrication strategies and smart-responsive behaviors to further improve the therapeutic efficacy of cancer.

In the present study, we have designed a tumor cell specific targeting nanocarrier consisted of DNA, protein and polysaccharide for combination of mRNA-responsive PDT and chemotherapy. This nanocarrier showed dual-targeted property, which combines the active targeting to cancer cell with intracellular tumor-related mRNA triggered drug release and PS activation. The final designated nanocomplex is comprised of three distinct functional elements: an mRNA responsive molecular beacon (MB) with drug and PS, protamine and hyaluronic acid (HA). As shown in Fig. 1A, a Ce6 (as PS) and BHQ2 (as quencher) labelled MB was utilized as drug carrier, the stem region of MB with GC pairs was used for loading of doxorubicin (DOX) and the loop portion of the MB was designed as recognition element of tumor-related mRNA. HA is known as an active tumor-targeting ligand to cell surface receptor of CD44 molecules, which are overexpressed in many tumors.[22] As shown in Fig. 1C, after targeted internalization by

[a] The United Innovation of Mengchao Hepatobiliary Technology Key Laboratory of Fujian Province, Mengchao Hepatobiliary Hospital of Fujian Medical University, Fuzhou 350025, P. R. China.
[b] The Liver Center of Fujian Province, Fujian Medical University, Fuzhou 350025, P. R. China.
[c] Fujian Institute of Research on the Structure of Matter, Chinese Academy of Sciences, Fuzhou, Fujian 350002, P. R. China.
[d] Liver Disease Center, The First Affiliated Hospital of Fujian Medical University, Fuzhou 350005, P. R. China.
Corresponding authors: E-mail Address: xiaoloong.liu@gmail.com Or E-mail Address: drjingfeng@126.com.
†Electronic Supplementary Information (ESI) available: Experimental details and supporting figures and tables. See DOI: 10.1039/x0xx00000x

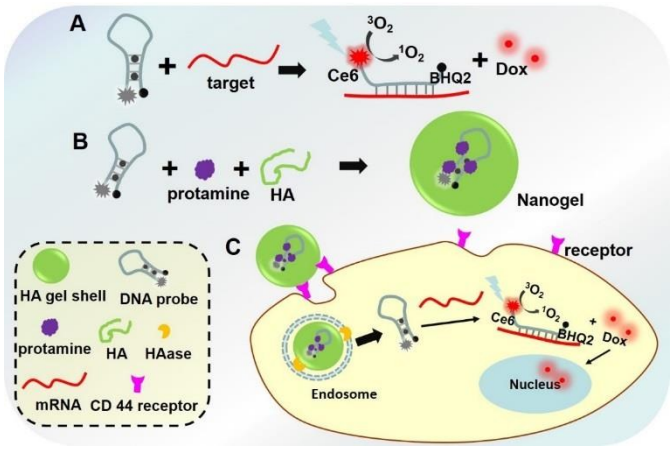

Fig. 1 Schematic illustration of the design and intracellular release of tumor mRNA-triggered smart nanodrug. (A) Mechanisms of target triggered release of Dox and activation of PDT. (B) Schematic illustration of the construction of nanocomplex. (C) Schematic illustration of cancer cell targeting and tumor mRNA triggered chemotherapy and PDT.

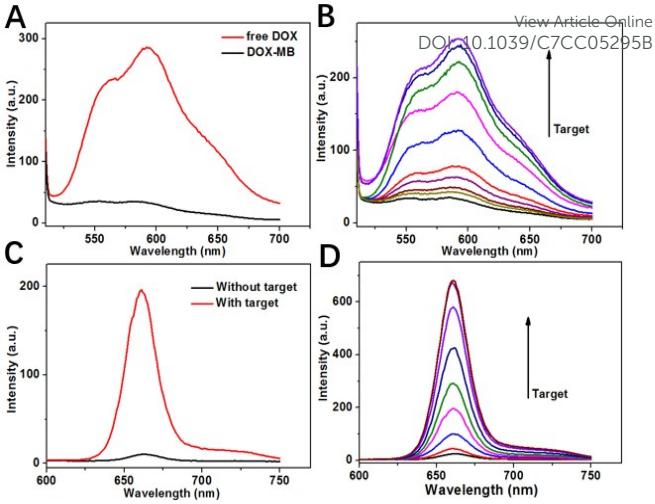

Fig. 2 (A) The fluorescence spectra of free Dox solution or DOX-MB (DOX loaded into the DNA duplex). λex = 485 nm. (B) The fluorescence spectra of DOX-MB in the presence of different concentrations of targets (0, 25, 50, 100, 150, 200, 300, 400, 500, 750 nM). (C) The fluorescence spectra of Ce6-BHQ2-MB with and without targets. λex = 404 nm. (D) The fluorescence spectra of Ce6-BHQ2-MB in the presence of different concentrations of targets (0, 25, 50, 100, 150, 200, 300, 400, 500 nM).

tumor cells, the HA shell of nanocomplex was degraded by hyaluronidase (HAase) and the cationic complexes were then released to facilitate intracellular delivery. Afterwards, the MB hybridized with the target to release the DOX and PS. Then the fluorescence and cytotoxicity of Dox were recovered and the ROS generation ability of Ce6 was also activated for PDT upon laser irradiation.

The intracellular TK1 mRNA was chosen as target, which is associated with cell division and proposed to be a biomarker for tumor growth.[23] Firstly, the Ce6 was covalently linked to the amino group at the 5' end of MB and the 3' end of MB was conjugated with BHQ2 as energy acceptor to quench the Ce6 and minimize its none-specific phototoxicity before activation by targets (named as Ce6-BHQ2-MB), and the UV-vis and MS spectra confirmed the successfully linkage of Ce6 and BHQ2 (Fig. S1A and Fig S2, ESI). After DOX intercalation into duplex, the characteristic absorption peak exhibited in the MB (named as DOX-MB) (Fig. S1B, ESI). Similarly, the fluorescence of DOX was also quenched by self-aggregation when loaded into the duplex (see Fig. 2A). The hybridization of DOX-MB with target DNA led to the release of DOX, which can be evaluated by the fluorescence recovery of DOX. As shown in Fig. 2B and Fig. S3A (ESI†), the recovered fluorescence is positively correlated with the increase concentration of targets. In the meantime, the quenched fluorescence of Ce6 in Ce6-BHQ2-MB also showed a remarkable recovery in the presence of targets (Fig. 2C). The fluorescence recovery showed a target concentration dependent manner (Fig. 2D and Fig. S3B, ESI†). Roughly about 70% of MBs were opened upon target binding, which can be calculated by comparing the recovered fluorescence of DOX or Ce6 with standard calibration curve (Fig. S4 and S5, ESI†). By comparison, the nontargets did not show obviously changes (Fig. S6, ESI). Thus, activation of Ce6 and DOX can be triggered specifically by the specific targets.

Next, the singlet oxygen generation ability of Ce6-BHQ2-MB toward DNA target was determined by ROS indicator (9,10-anthracenediyl-bis(methylene) dimalonic acid, ABDA). In the absence of target, because of the efficient quenching of Ce6 by BHQ2, the ABDA absorbance did not show significant decrease upon laser irradiation at 670 nm (Fig. S7, ESI). However, the ROS generation ability of Ce6 was recovered when incubated with DNA target, and the ABDA absorbance decreased continuously along with time under laser irradiation (Fig. S8, ESI). This result indicated that the ROS generation of Ce6-BHQ2-MB can be specifically activated by its target. Taken together, our designed strategy can be used to effectively release DOX and activate Ce6 via target DNA hybridization, which provides a foundation for the construction of mRNA responsive DDS.

HA, a polyanion polysaccharide with excellent biocompatibility and biodegradability, has been used as a promising carrier candidate and tumor-targeting moiety for intracellular delivery of various therapeutic agents.[24,25] Protamine is a nontoxic, positively charged and naturally occurring polypeptide, and has be used as a condensing agent for oligodeoxynucleotide and as a nanocarrier for gene delivery.[26] These two opposite charge polyelectrolytes can form nanocomplexes by a facile electrostatic interaction-mediated self-assembly approach. The mass ratio of HA to protamine has important influence on the diameter and surface charge of the resulting nanocomplex (HA-Pro). The relationship between the weight ratios and physicochemical properties of HA-Pro nanocomplex was summarized in Table S1 (ESI†). When the mass ratio was set as 2:1, the nanocomplex has an average size of ~150 nm, zeta potentials of -29.9 mV and polydispersity index (PDI) of 0.09. At this weight ratio, the nanocomplex has a suitable particle size for cell application and a negative surface charge (HA shell outside) for cancer cell targeting. The encapsulation doses of Ce6-BHQ2-DOX-MB into the nanocomplex (named as HA-Pro-Ce6-DOX) were also optimized (see Table S2, ESI), and 10 μM Ce6-

BHQ2-DOX-MB were chosen for the self-assembly of DNA-nanocomplex. As shown in Fig. S9A and S9B (ESI†), the obtained nanocomplex has a zeta potential of –30 mV and an average size of 155 nm. The transmission electron photomicrographs (TEM) showed a spheroid structure of the nanocomplex (Fig. S9C, ESI). High loading efficiency of DNA complexes into the nanocomplex was further confirmed by electrophoresis assay (Fig. S9D, ESI). Compared to free form of DNA (lane1), the migration of DNA in nanocomplex was efficiently prevented (lane 2) and reappeared after treatment with 2% SDS prior to electrophoresis (lane 3).

The nuclease stability of DNA based nanocarrier is an important property for imaging and therapeutic applications in living cells. As shown in Fig. S10 (ESI†), compared with the free DNA, the encapsulated DNA in nanocomplex was protected from degradation and remained stable after treatment with enzyme deoxyribonuclease I (DNase I) for 2 h. This revealed that the nanocomplex possessed high resistance to the nuclease and suitable for cell applications.

To demonstrate HA degradation by HAase, the change of zeta potential of nanocomplex was examined after incubation with HAase at different pH values over time (Fig. S11, ESI†). The zeta potential of nanocomplex changed from highly negative (-29.4 mV) to less negative (-5 mV) after exposure to HAase at pH 7.4 for 2 h. Moreover, the zeta potential further rose to +1 mV when incubated at pH 5.5, because the acidic condition can accelerate degradation of nanocomplex and improve the HAase activity. In addition, the abundant HAase in cytosol of tumor cells can improve the release of DNA from nanocomplex upon cellular uptake and increase the therapeutic efficacy. The target triggered release of DOX and activation of Ce6 after HA degradation by HAase was further investigated. As shown in Fig. S12 (ESI†), in the presence of HAase and target, the release rate and released content of DOX from drug loaded MB were dramatically accelerated. However, in the absence of HAase or target, the DOX release was obviously reduced. Meanwhile, the fluorescence recovery of Ce6 also showed similar responsive behaviors. These results further revealed that the release of DOX and Ce6 was indeed due to the hybridization with its corresponding targets.

To assess the targeted ability of the nanocomplex in living cells, three different cell lines were chosen: the cervical cancer cell line (HeLa) as experimental cells where the HA receptor (CD44) and TK1 mRNA were both overexpressed[17,27], while the mouse embryonic fibroblast cells (NIH3T3) and the Human umbilical vein endothelial cells (HUVEC) as control normal cells where the HA receptor (CD44) was negative[28]. As shown in Fig. 3A, the nanocomplex selectively internalized into the HeLa cells, and an obvious red fluorescence signal of Ce6 and a green fluorescence signal of DOX can be clearly observed by confocal laser scanning microscopy (CLSM). While very weak signals were observed in both NIH3T3 cells (Fig.3B) and HUVEC cells (Fig.S13, ESI†) under the same conditions, which due to the absence or very low expression of the HA receptors (CD44). Moreover, the HeLa cells pre-treated with excess of free HA, the cellular uptake of nanocomplex was drastically inhibited, and the fluorescence signals of Ce6 and DOX can hardly be seen (Fig. 3C). Furthermore, the TK1 mRNA expression in HeLa cells was down-regulated with tamoxifen and up-regulated with beta-estradiol[17]. The results clearly showed that the fluorescence intensities of Ce6 and Dox both increased in the beta-estradiol treated cells as the upregulated expression of TK1 mRNA level and decreased fluorescence intensities in the tamoxifen treated cells since the downregulated TK1 mRNA expression (Fig. S14, ESI†). These results suggested that the dual-targeted nanocomplex preferentially internalized into specific cancer cells due to the presence of HA receptors, and released DOX and activated Ce6 selectively in cancer cells after hybridization with intracellular TK1 mRNA targets.

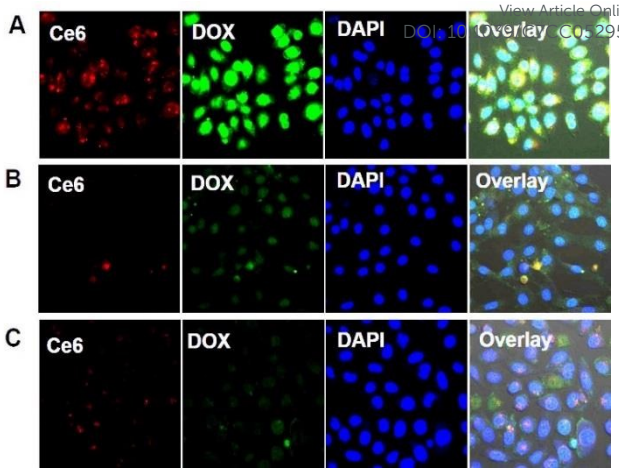

Fig. 3 Intracellular delivery of HA-Pro-Ce6-DOX observed by CLSM. (A) Hela cells, (B) NIH 3T3 cells and (C) Hela cells pre-treatment with 10 mg·mL^{-1} of HA.

After confirming the dual-targeting ability of nanocomplex, the ROS generation ability in living cells was examined. The 2,7-dichlorodihydrofluorescein diacetate (DCF-DA) was used as the intracellular ROS-detecting probe. As shown in Fig. S15 (ESI†), after incubation with the PS loaded nanocomplex, the cells showed very weak green fluorescence before laser irradiation, indicating that a relatively less amount of ROS was produced. However, a strong green fluorescence was clearly observed when the cells incubated with PS loaded nanocomplex and irradiated by laser. As a control, the nanocomplex without loading of Ce6-BHQ2-MB or the nanocomplex formed by the control MB (named as Ce6-BHQ2-cMB) with mismatched sequence, did not show obvious ROS production either with or without laser irradiation (Fig. S15 and Fig. S16, ESI†). These results confirmed that the nanocomplex can be an effective responsive PS in target cells.

Furthermore, the combined therapeutic effects of nanocomplex was investigated by CCK-8 assay. Cells in darkness without nanocomplex treatment was set to the viability of 100% as a reference. As shown in Fig. 4A-1 and 4B-1, both the cancer cells and normal cells showed slight cytotoxicity after laser irradiation, indicating that the laser irradiation alone has no damage effects. Blank nanocomplex without drug also has no cytotoxicity under laser irradiation (Fig. 4A-2 and 4B-2). When the cancer cells were incubated with HA-Pro-Ce6 nanocomplex (without DOX), the PDT alone led to 48% of cell death (Fig. 4A-3); and the chemotherapy

alone (incubated with HA-Pro-DOX-MB, under dark) led to 64% of cell death (Fig. 4A-4, red bar). Strikingly, under the combination of PDT and chemotherapy, the viability of HeLa cells dropped significantly down to 15% (Fig. 4A-4, black bar). In comparison, the drug loaded nanocomplex showed lower therapeutic effects toward NIH3T3 cells under similar conditions of single modal or combined therapy (Fig. 4B-3/4) for lacking targeting receptors.

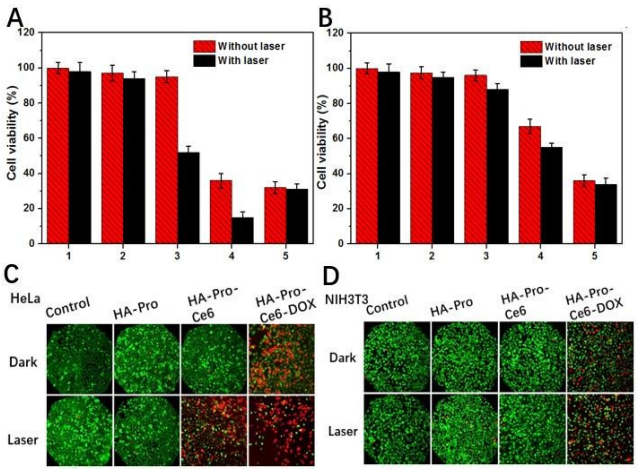

Fig. 4 In vitro cytotoxicity of 1) Control, 2) HA-Pro, 3) HA-Pro-Ce6, 4) HA-Pro- Ce6-DOX and 5) free DOX toward HeLa (A) and NIH3T3 (B) cells with and without 670 nm laser irradiation. Error bars indicate s.d. (n=4); LIVE/DEAD cell viability of HeLa cells (C) and NIH3T3 (D) treated without or with HA-Pro, HA-Pro-DNA-Ce6 and HA-Pro-DNA-Ce6-DOX. Viable cells were stained green with Calcein AM, dead cells were stained red with EthD-1.

Furthermore, the synergistic therapeutic efficacy of the nanocomplex was also analysed by LIVE/DEAD (green/red) staining assay. As expected, almost all cancer cells were killed after the combination of PDT and chemotherapy, which was much better than single treatment (Fig. 4C); while the control cells under similar treatment showed no significant cell killing activities. Thus, the dual targeted nanocomplex via cancer cell specific targeting and tumor-related mRNA activated response could serve as an effective platform for combination of PDT and chemotherapy against cancer with minimized side effects.

In summary, a novel and effective dual-targeted nanocomplex has been developed for combination of PDT and chemotherapy to against cancer cells. This nanocomplex was fabricated by a self-assembly approach with drug loaded DNA, protein and polysaccharide, which showed active targeting ability to cancer cells and intracellular tumor-related mRNA triggered drug release and PS activation. The enhanced therapeutic efficacy of our smart nanocomplex to specifically against cancer cells has also been demonstrated. Therefore, the reported nanocomplex might be a promising candidate for targeted cancer therapy.

This work was supported by the National Natural Science Foundation of China (Grant No. 61575044, U1505221, 81671813, and 21605021); the Joint Funds for the innovation of science and Technology of Fujian province (Grant No. 2016Y9060, and 2016Y9062); the Science and Technology Infrastructure Construction Program of Fujian Province (Grant No. 2014Y2005); the Natural Science Foundation of Fujian Province of China (Grant No. 2016J05206 and 2016J05207); Youth Scientific Research Subject of Fujian Provincial Health and Family Planning Commission (Grant No. 2016-1-85); the Science and Technology Planning Project of Fuzhou (Grant No. 2016-S-124-8 and 2016-S-124-13) and the Startup Fund of Mengchao Hepatobiliary Hospital of Fujian Medical University (Grant No.QDZJ-2016-003).

Notes and references

1 D. E. J. G. J. Dolmans, D. Fukumura and R. K. Jain, *Nat. Rev. Cancer*, 2003, **3**, 380–387.
2 Z. Zhou, J. Song, L. Nie and X. Chen, *Chem. Soc. Rev.*, 2016, **45**, 6597–6626.
3 B. Tian, C. Wang, S. Zhang, L. Feng and Z. Liu, *ACS Nano*, 2011, **5**, 7000–7009.
4 B. Jang, J. Y. Park, C. H. Tung, I. H. Kim and Y. Choi, *ACS Nano*, 2011, **5**, 1086–1094.
5 Y. Lu, A. A. Aimetti, R. Langer and Z. Gu, *Nat. Rev. Mater.*, 2016, **2**, 16075.
6 V. P. Torchilin, *Nat. Rev. Drug Discov.*, 2014, **13**, 813–827.
7 S.-W. Choi, Y. Zhang and Y. Xia, *Angew. Chemie Int. Ed.*, 2010, **49**, 7904–7908.
8 R. Tong, H. H. Chiang and D. S. Kohane, *Proc. Natl. Acad. Sci.*, 2013, **110**, 19048–19053.
9 Y. Wang, S. Song, J. Liu, D. Liu and H. Zhang, *Angew. Chemie - Int. Ed.*, 2015, **54**, 536–540.
10 C. E. Callmann, C. V. Barback, M. P. Thompson, D. J. Hall, R. F. Mattrey and N. C. Gianneschi, *Adv. Mater.*, 2015, **27**, 4611–4615.
11 J. Li, S. Wu, C. Wu, L. Qiu, G. Zhu, C. Cui, Y. Liu, W. Hou, Y. Wang and L. Zhang, *Nanoscale*, 2016, 8600–8606.
12 Y. Ma, Z. Wang, M. Zhang, Z. Han, D. Chen, Q. Zhu, W. Gao, Z. Qian and Y. Gu, *Angew. Chemie Int. Ed.*, 2016, **55**, 3304–3308.
13 J. Liu, L. Zhang, J. Lei, H. Shen and H. Ju, *ACS Appl. Mater. Interfaces*, 2017, **9**, 2150–2158.
14 H. Schwarzenbach, D. S. B. Hoon and K. Pantel, *Nat Rev Cancer*, 2011, **11**, 426–437.
15 W. Pan, Y. Li, M. Wang, H. Yang, N. Li and B. Tang, *Chem. Commun.*, 2016, **52**, 4569–4572.
16 Y. Yang, J. Huang, X. Yang, K. Quan, H. Wang, L. Ying, N. Xie, M. Ou and K. Wang, *J. Am. Chem. Soc.*, 2015, **137**, 8340–8343.
17 W. Pan, H. Yang, T. Zhang, Y. Li, N. Li and B. Tang, *Anal. Chem.*, 2013, **85**, 6930–6935.
18 D. Wu, G. Song, Z. Li, T. Zhang, W. Wei, M. Chen, X. He and N. Ma, *Chem. Sci.*, 2015, **6**, 3839–3844.
19 C. Lu, C. Zhu, J. Li, J. Liu, X. Chen and H.-H. Yang, *Chem. Commun.*, 2010, **46**, 3116.
20 T. Chen, C. S. Wu, E. Jimenez, Z. Zhu, J. G. Dajac, M. You, D. Han, X. Zhang and W. Tan, *Angew. Chemie - Int. Ed.*, 2013, **52**, 2012–2016.
21 K. Ke, L. Lin, H. Liang, X. Chen, C. Han, J. Li and H.-H. Yang, *Chem. Commun.*, 2015, **51**, 6800–6803.
22 M. Götte and G. W. Yip, *Cancer Res.*, 2006, 66, 10233–10237.
23 C. C. Chen, T. W. Chang, F. M. Chen, M. F. Hou, S. Y. Hung, I. W. Chong, S. C. Lee, T. H. Zhou and S. R. Lin, *Oncology*, 2007, **70**, 438–446.
24 S. Wang, M. Cao, X. Deng, X. Xiao, Z. Yin, Q. Hu, Z. Zhou, F. Zhang, R. Zhang, Y. Wu, W. Sheng and Y. Zeng, *Adv. Healthc. Mater.*, 2015, **4**, 281–290.
25 R. Mo, T. Jiang, R. DiSanto, W. Tai and Z. Gu, *Nat. Commun.*, 2014, **5**, 3364.
26 F. Sorgi, S. Bhattacharya and L. Huang, *Gene Ther.*, 1997, **4**, 961–968.
27 M. Ma, H. Chen, Y. Chen, K. Zhang, X. Wang, X. Cui and J. Shi, *J. Mater. Chem.*, 2012, **22**, 5615–5621.
28 F. Li, S.-J. Park, D. Ling, W. Park, J. Y. Han, K. Na and K. Char, *J. Mater. Chem. B*, 2013, **1**, 1678–1686.